Ridges and hotspots: perspectives from global tomography

Yu-Shen Zhang and Toshiro Tanimoto

Seismological Laboratory 252-21
California Institute of Technology

Resolution in global tomography has improved to a level of about 1000 km due to a rapid increase of digital data during the last decade. We have started to see various important tectonic features in some detail. We will attempt to summarize our current observations for ridges and hotspots.

Depth cross-sections of our recent S-wave velocity results, perpendicular to three ridges, are shown in Figures 1. These are stacked sections over 30 degrees along the ridge axis and the axis is aligned at the center of the figures, denoted by arrows. The velocity scale (in percent) is given on the bottom of figures. Contours are at every 0.5 percent and patterns change every percent. The most notable feature in these figures is the concentration of very low velocity anomalies (less than -1 percent) in the top 100 km. The minimum velocity is shallower than 50 km. Ridges are located above slow velocity regions, but in general we cannot see any features which suggest active upwelling. The fastest spreading East Pacific Ridge does have a 0.5 percent contour which extends to about 200 km in depth, but this could be interpreted as induced upwelling due to very fast spreading.

S-wave velocity at four depths under the ridge axes as a function of spreading rate are shown in Figure 2. Depths vary from 36 to 100 km and the possible contaminations from hotspots and triple junctions are avoided. It is clear that the shallow results (36 and 60 km) strongly correlate with spreading rate, but correlations decrease for deeper results and vanish at 100 km. Melt fraction due to decompression melting should increase with spreading rate, thus this trend can be understood as simple decompression effects. Both Figures 1 and 2 suggest that ridges are mainly passive features, and faster spreading ridges tend to induce deeper upwelling currents.

On the other hand, low velocity anomalies associated with hotspots are relatively deep. Figure 3 shows our S-wave velocity at two major hotspots. We will show more results in the conference. They all show low velocity anomalies, but the minimum velocity is located typically between 100 and 200 km depths. Differences in depth from low velocity anomalies at ridges are clear. They suggest that plume heads are creating low velocity anomalies below the lithosphere. Stems of plumes are presumably narrower than our resolution (1000 km), thus making them impossible to detect in these plots.

From these observations, we make the following conjecture: the depth of the low velocity anomaly can serve as a criterion to distinguish the nature (passive or active) of upwelling. If it is shallow, a passive mechanism is suggested, while deep anomalies suggest active mechanisms. With this in mind, we created two cross-sections in North-East Africa (Fig. 4). One is along the Red Sea and the other is perpendicular to it and crosses the East African Rift. Note that the north and south ends are denoted in the figure, as well as the locations of the Red Sea. The Red Sea is associated with a low velocity anomaly as expected, but the anomaly is clearly deeper than those for ridges. Active upwelling is clearly indicated and furthermore, the shape of the low velocity anomaly suggests that materials may be fed by hotspots at the southern end (Afar). The cross-section for the East African Rift also suggests an active origin, fed by a deeper low velocity anomaly from the South-West (under Africa). These results may be a useful tool to identify origins of other continental rifts.

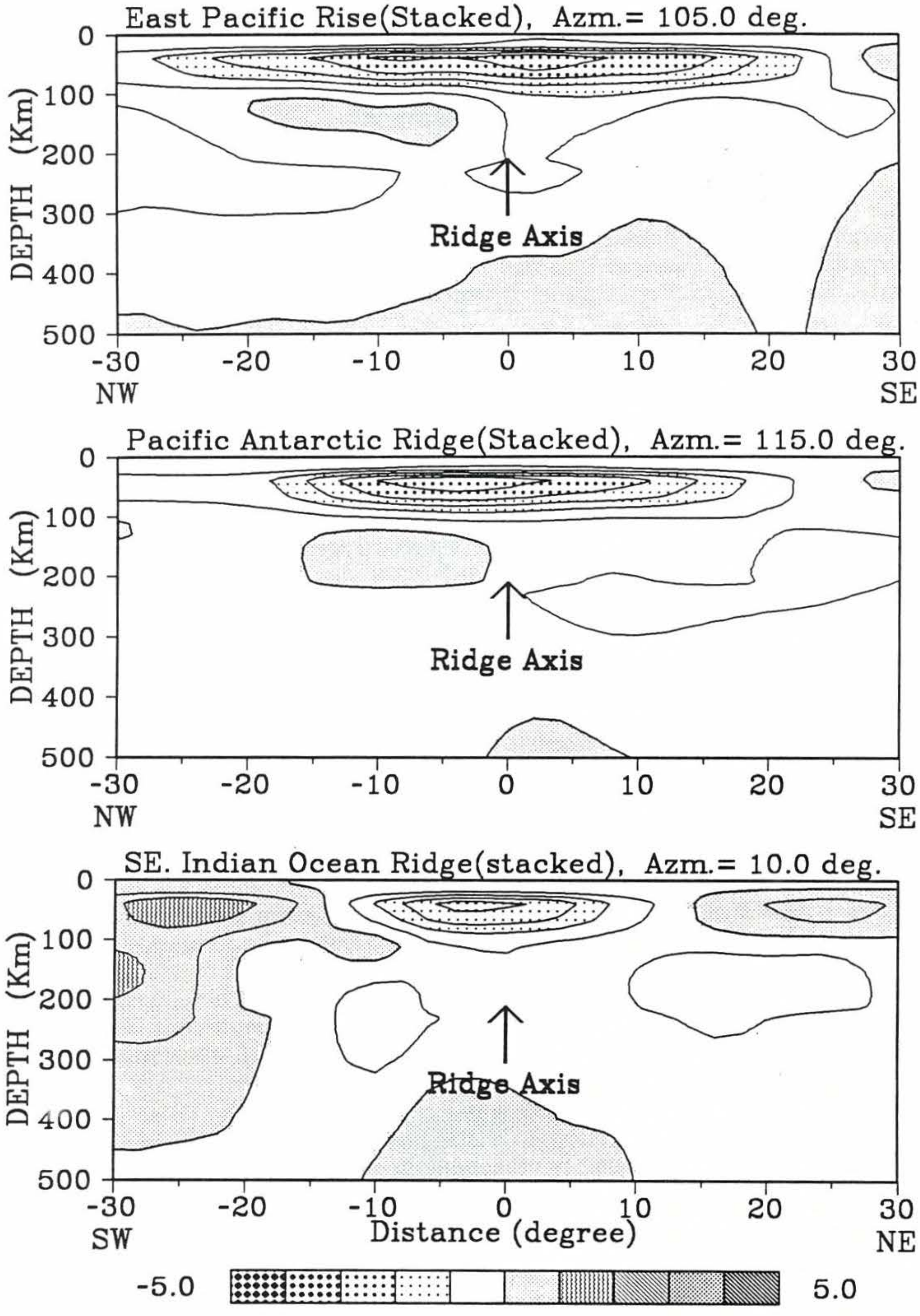

Fig. 1. Cross-sections of S-wave velocity results for East Pacific Rise, Pacific Antarctic Ridge and South-East Indian Ocean Ridge, respectively. These are stacked sections over 30 degrees along the ridge axis. The ridge axis is aligned at the center of the figure, denoted by arrow. The azimuth (clockwise from north) of each section is shown on top. The velocity contours are at 0.5 percent and patterns change every percent.

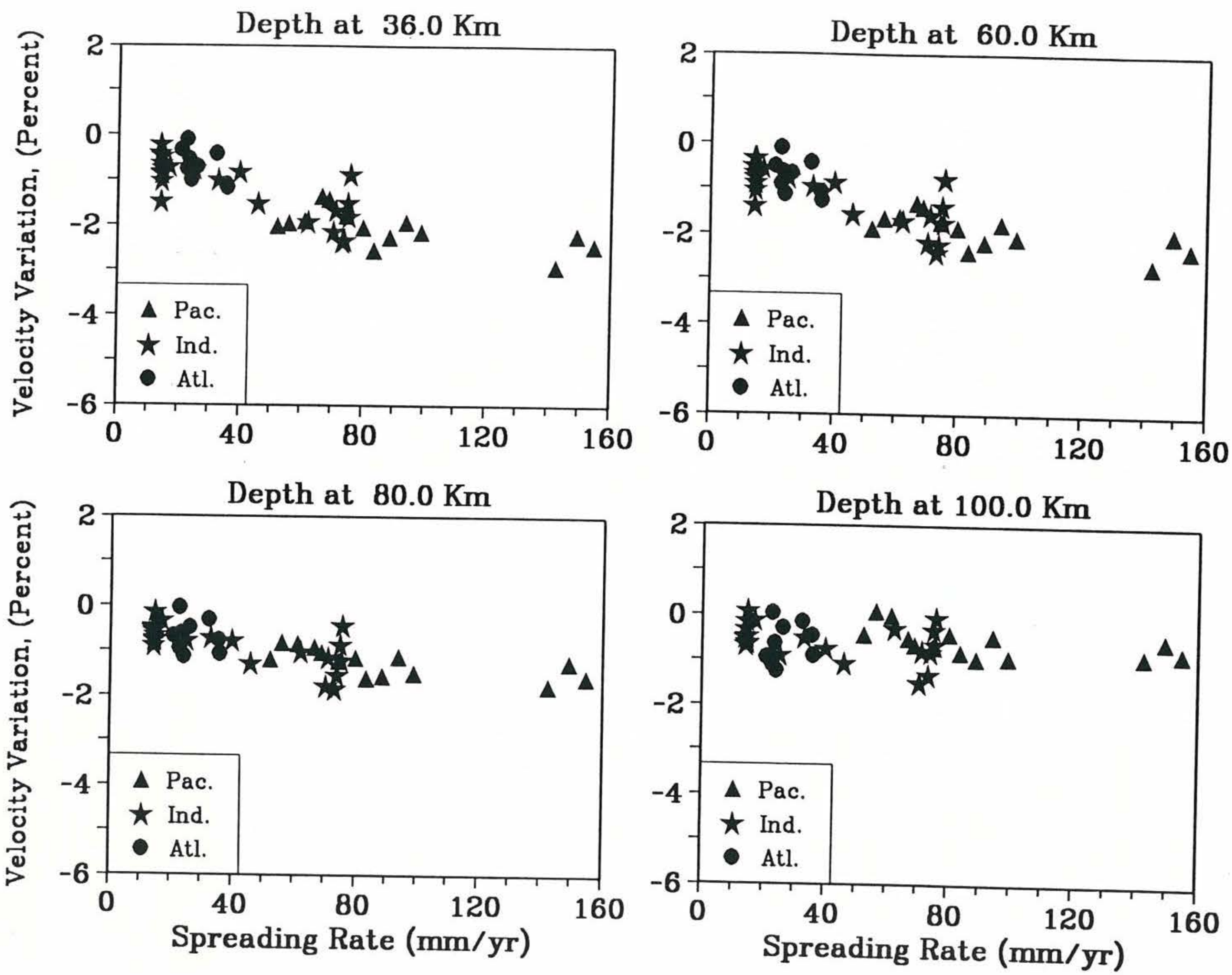

Fig. 2. S-wave velocity at four depths under the ridge axes as a function of spreading rate. Each point means an average velocity stacked over 8 degrees along the ridge axis. Different symbols are used to distinguish ridge in different oceans.

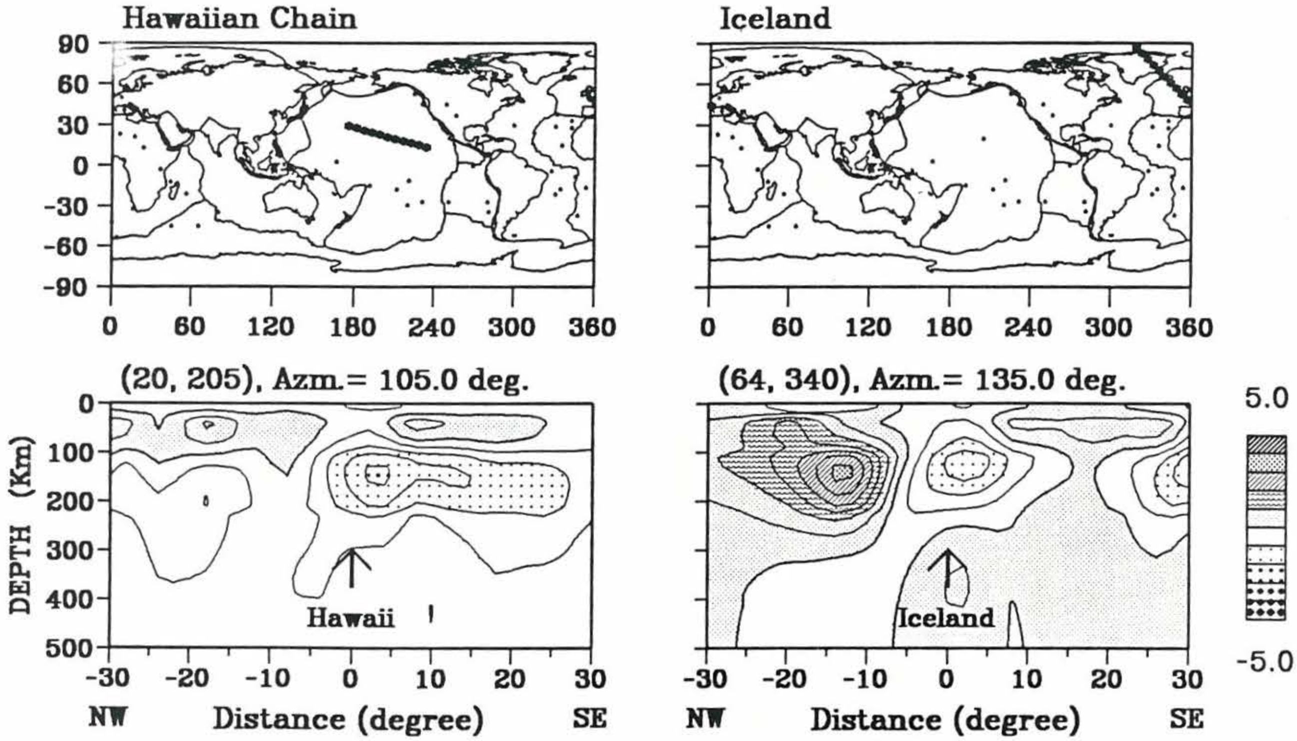

Fig. 3. Lower parts are two vertical cross-sections of S-wave velocity results at Hawaii and Iceland hotspots. The latitude, longitude of the center point, and the azimuth of the cross line are given in the figures. The directions of the line are also shown at bottom. Top parts give locations of the cross lines (star line). The velocity scale is same as in Figure 1.

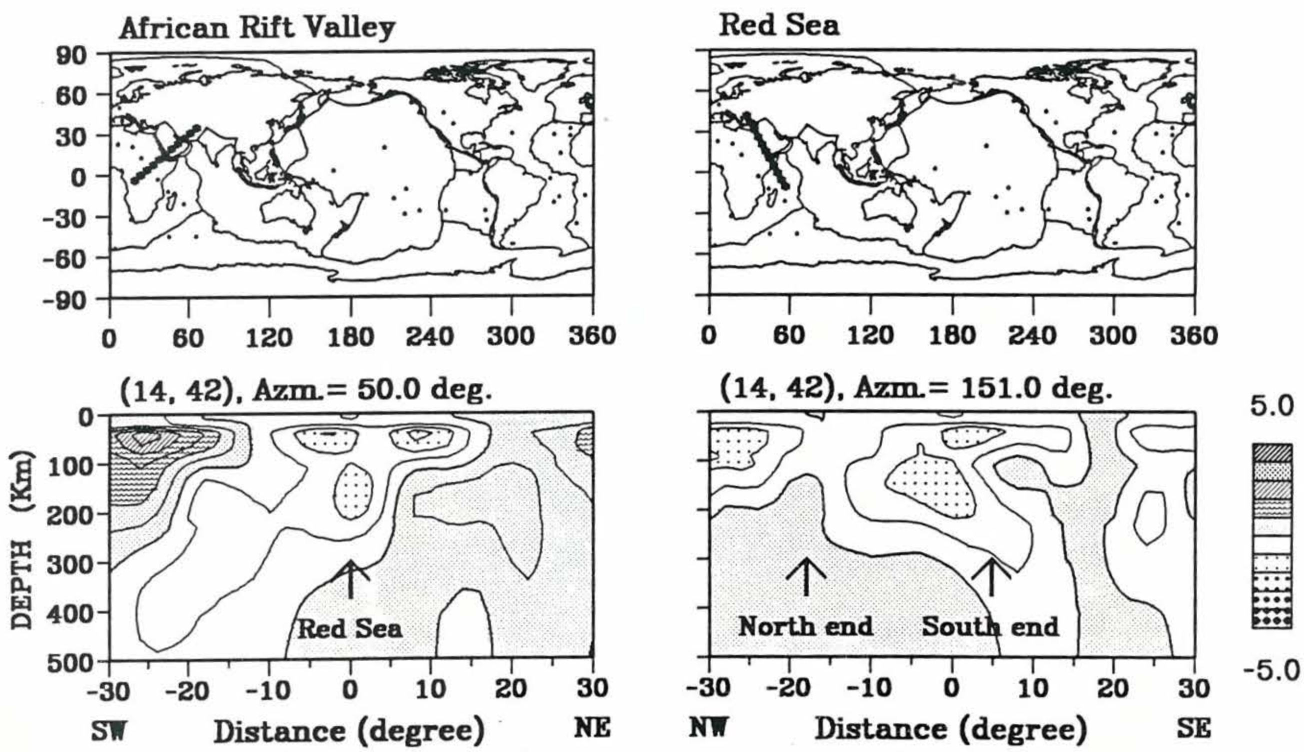

Fig. 4. The same as Figure 3 but for African Rift Valley and Red Sea cross-sections. These two cross-sections are almost perpendicular.

1991 PLUME SYMPOSIUM

CALTECH

10^{-7} Æ